Urolithiasis (2015) 43:397–409
DOI 10.1007/s00240-015-0781-5

ORIGINAL PAPER

Exploring calcium oxalate crystallization: a constant composition approach

Ann M. Kolbach-Mandel[2] · Jack G. Kleinman[2] · Jeffrey A. Wesson[1,2]

Received: 12 January 2015 / Accepted: 6 May 2015 / Published online: 28 May 2015

Abstract Crystal growth rates have been extensively studied in calcium oxalate monohydrate (COM) crystallization, because COM crystals are the principal component in most kidney stones. Constant composition methods are useful for studying growth rates, but fail to differentiate concurrent nucleation and aggregation events. A constant composition method coupled with particle size determinations that addresses this deficiency was previously published for a calcium phosphate system, and this method was extended to COM crystallization in this report. A seeded constant composition experiment was combined with particle size determination and a separate near-equilibrium aggregation experiment to separate effects of growth rate, nucleation, and aggregation in COM crystal formation and to test the effects of various inhibitors relevant to stone formation. With no inhibitors present, apparent COM growth rates were heavily influenced by secondary nucleation at low seed crystal additions, but growth-related aggregation increased at higher seed crystal densities. Among small molecule inhibitors, citrate demonstrated growth rate inhibition but enhanced growth-related aggregation, while magnesium did not affect COM crystallization. Polyanions (polyaspartate, polyglutamate, or osteopontin) showed strong growth rate inhibition, but large differences in nucleation and aggregation were observed. Polycations (polyarginine) did not affect COM crystal growth or aggregation. Mixtures of polyanions and polycations produced a complicated set of growth rate, nucleation, and aggregation behaviors. These experiments demonstrated the power of combining particle size determinations with constant composition experiments to fully characterize COM crystallization and to obtain detailed knowledge of inhibitor properties that will be critical to understanding kidney stone formation.

Keywords Nephrolithiasis · Calcium oxalate · Crystal aggregation · Constant composition · Crystal inhibitors · Osteopontin

Introduction

Sparingly soluble salts of calcium have been studied with respect to pathological crystallization like kidney stones (calcium oxalates) [1, 2], and physiologic crystallizations such as bone and tooth mineralization (calcium phosphates) [3, 4] or marine exoskeletal systems and egg shells (calcium carbonate) [3, 5, 6]. These studies have been pursued with several approaches including batch nucleation and seeded methods. Crystallization of supersaturated solutions has been initiated either by the addition of preformed seed crystals or as a result of spontaneous nucleation and depletion of the reactants. In a careful review of calcium oxalate crystallization methods, Kavanagh [7] describes the inherent drawback of the continually changing solution saturation levels and the inability to maintain steady state in batch methods such as these. Two current approaches to crystallization that address this problem are mixed suspension mixed product removal (MSMPR) and constant composition methodologies.

MSMPR systems, also known as stone farms, begin with a nucleating surface with constant replacement of the

✉ Jeffrey A. Wesson
jwesson@mcw.edu

[1] Department of Veterans Affairs Medical Center, 5000 W National Avenue (111K), Milwaukee, WI 53295, USA

[2] Department of Medicine/Nephrology, Medical College of Wisconsin, 9200 W Wisconsin Avenue, Milwaukee, WI 53226, USA

crystallization solution; stable supersaturation conditions can be maintained over the course of days and have resulted in production of in vitro stone-like masses [8]. While the method can determine the effects of various constituents of urine or additives on the bulk growth of stone material, there are some significant limitations. Aside from the considerable length of time, from days to weeks, it takes to determine the effect of an additive on crystal growth; the method requires large volumes (1 L/day) of feed solutions thus limiting its utility in assessing macromolecules that are in limited supply. The method does, however, routinely utilize particle sizing of the suspension to separate the effects of nucleation and aggregation from growth of preformed stone cores.

The constant composition (CC) method monitors calcium loss with a calcium sensitive electrode and replaces ions lost from the solution to the growing crystal surface by titration. CC was first introduced in 1978 to study hydroxyapatite crystallization [9, 10]. Since its introduction, the assay has been used to study not only hydroxyapatite crystallization [11–15], but also other calcium salts, including octacalcium phosphate [16], calcium fluoride [17], calcite [18–20], and calcium oxalate [21–24].

As noted in earlier research, overall stone or crystal mass growth rate is an insufficient parameter to describe the concurrent crystallization processes of growth, aggregation, and nucleation [7, 25, 26]. In earlier work, we demonstrated supplementing the constant composition technique with particle size distribution (PSD) analysis to study hydroxyapatite crystallization. These experiments revealed that secondary nucleation (i.e., the creation of new, smaller crystals triggered by the presence of preexisting crystal surfaces) and aggregation during growth, that we refer to as growth-related aggregation (i.e., the fusion of newly formed or preexisting crystals and aggregates into yet larger aggregates) were occurring in addition to simple growth of preformed crystals [11]. We also showed that low seed crystal additions favor secondary nucleation, while higher seed crystal additions favor growth-related aggregation. Thus, in this paper, we will refer to the data derived from the constant composition approach, as the apparent (crystal) growth rate to signify that additional processes were responsible for the rates of calcium consumption observed. The current study on calcium oxalate (CaOx) crystallization applies similar methodologies and combines the data from constant composition and static calcium oxalate monohydrate (COM) aggregation studies [27] to yield a clearer understanding of the formation of COM than is provided by any either technique alone, specifically including information on processes of aggregation and nucleation. In addition, these investigations include studies of the effects of various inhibitors on COM formation, based on our interest in the fundamental processes underlying kidney stone formation.

Stone disease, which affects 10 % of the general population, is dependent on the crystallization of inorganic components, predominantly calcium oxalate, from supersaturated urine. A greater insight into the principles underlying CaOx crystallization will be invaluable in discerning and preventing the processes that result in stone formation. Urine macromolecules have been known to be modulators of CaOx crystallization processes for many years [28–30]. The homopolymers of aspartate, glutamate, and arginine along with the urinary protein osteopontin were tested in the current study to model the effects of urine macromolecules on COM formation. Also, citrate and magnesium were tested to discern how small molecule inhibitors in urine affect the CaOx crystallization process.

Materials and methods

COM seed crystal preparation

Calcium oxalate monohydrate seed crystals were prepared by the drop-wise addition of 10 mM solutions of $CaCl_2$ and $Na_2C_2O_4$ at room temperature (4 L total volume, mixed 1 week). The crystals were allowed to settle by gravity, supernatant aspirated, and recovered by low speed centrifugation. Crystals were washed twice with methanol and dried at 65 °C. X-ray powder diffraction confirmed the composition (VA National Crystal Identification Center, Milwaukee, WI, USA), and the surface area was measured using gas adsorption (1.5 m^2/g). Crystals used in the following crystal assays were brought up as a slurry (1.5 mg/mL) in HEPES buffer (10 mM HEPES, 150 mM NaCl, pH 7.5), which would rapidly (few hours) became saturated with respect to CaOx through dissolution of a small amount of COM crystals. The resulting suspension was allowed to stir a minimum of 3 weeks prior to use, to allow stabilization of the surface properties through equilibration processes, which reduced variability in growth rate measurements between different aliquots from this seed batch.

Calcium oxalate aggregation assays (AA-COM)

Static COM seed crystal aggregation was assessed as previously described [27]. Briefly, metastable solutions of calcium and oxalate (0.25 mM CaOx, $\sigma = 0.27$) in HEPES buffer were allowed to incubate with and without crystallization modifiers added for 15 min at 37 °C. COM crystals, 300 µg, were added and mixed for 1 h. Particle size, Dw, was measured on the seed crystal after 1 h to assess the level of disaggregation or aggregation promotion. Relative supersaturation, σ, was calculated using SPEC96 software (a kind gift from G. Nancollas). In this formulation, undersaturation would be indicated by a negative value and supersaturation by a positive one. The conditions used in these studies, representing slight supersaturation,

were chosen to prevent dissolution of the seed crystals, as described previously [27].

Constant-composition COM seeded apparent crystal growth assays (CC-COM)

In a thermostatted reaction vessel (37 °C, 5 mL), 0.5 mM $CaCl_2$ and $Na_2C_2O_4$ in HEPES buffer were allowed to equilibrate for 20 min prior to seed crystal addition. A calcium ion selective electrode (Radiometer Analytical) was used to monitor calcium ion concentration using a pH meter (pH713, Brinkman). Constant composition was maintained using two DU765 Dosimats (Brinkman), one with 5 mM $CaCl_2$ and the other with 5 mM $Na_2C_2O_4$ in a HEPES buffer solution. The instruments were controlled and data acquired using LabVIEW software (National Instruments). The reaction was considered complete at the mass doubling point, when the titrant addition effectively equaled the mass of the added seed crystal. Choice of this extent of reaction as a termination point was somewhat arbitrary, but it provided a consistent way to compare growth rates at conditions with differing growth profiles, some of which deviated strongly from linearity. The average growth rate, m, is calculated by dividing the μmoles COM formed by the time to reaction completion. Apparent growth rate inhibition is reported as percent inhibition relative to a control rate of the same seed crystal addition, described as.

$$\%\ \text{Inh} = \left(\frac{m\text{CONT} - m\text{Sample}}{m\text{CONT}}\right) \times 100,$$

where m = calculated growth rate (μg/min). All reactions were performed at $\sigma = 1.42$.

Particle size distribution analysis

Particle size distribution (PSD) analysis was performed on COM seed crystal slurries using an Accusizer 780 (Particle Sizing Systems). Particle size was immediately assessed on aggregation assay (AA-COM) and constant-composition (CC-COM) samples post assay by dispersing 100–300 μl of reaction sample into 15 mL sizing buffer (0.225 mM in $CaCl_2$ and $Na_2C_2O_4$, 150 mM NaCl, and HEPES buffer). The sizing buffer concentration was empirically determined to be the solution condition where no growth or dissolution occurred in 1 h. The weight averaged particle diameter, Dw, was used to calculate the ratio of diameters, Rd, comparing the final diameter to the initial seed crystal diameter. The ratio of diameters for the aggregation assay, Rd(AA), is described as

$$\text{Rd(AA)} = \frac{\text{Dw (final)}}{\text{Dw (COM seed)}}$$

The effect of any additive on the equilibrium COM PSD could thereby be rated as either inert (Rd(AA) = 1), aggregating (Rd(AA) > 1), or disaggregating (Rd(AA) < 1) of preformed COM crystals in this static crystal assay (AA-COM).

Ideal crystal growth rate is based on the assumptions that all newly formed crystalline material is applied directly to the surface of the seed crystal and that all crystal surfaces grow at the same rate. The Rd values used in the CC assay require normalization based not on the initial COM seed crystal distribution, but on an estimated mass-doubled profile (IDEAL) resulting from crystal growth of the preformed seed crystals under ideal conditions [11]. The ratio of diameters for the constant composition assay, Rd(CC), was defined as.

$$\text{Rd(CC)} = \frac{\text{Dw (final)}}{\text{Dw (IDEAL)}}$$

Evidence of the growth-related processes of secondary nucleation or growth-related aggregation could then be discerned by comparing Rd(CC) to Rd(AA), since the effect of any additive on the equilibrium PSD must first be included in the comparison. In a pure growth system, Rd(AA) = Rd(CC), but growth-related aggregation would be indicated by particles made bigger than expected (Rd(CC) > Rd(AA)) by fusing crystals and aggregates, while secondary nucleation would be indicated by finding smaller than expected particles (Rd(CC) < Rd(AA)) from secondary nucleation of new, smaller crystals. To better illustrate this analysis, consider an experimental condition where Rd(CC) = 1. If Rd(AA) = 1 for a particular experimental condition, then Rd(CC) = 1 would indicate pure growth for that condition, because the particles were of the expected size. However, if Rd(AA) < 1 due to an equilibrium disaggregating effect of an additive, then the finding of Rd(CC) = 1 would indicate growth-related aggregation, because the particles were bigger than expected for this condition (Rd(CC) > Rd(AA)). Alternatively, if Rd(AA) > 1 due to additive-induced aggregation at equilibrium, then Rd(CC) = 1 would indicate secondary nucleation, since the particles were smaller than expected (Rd(CC) < Rd(AA)).

Further evidence of nucleation or growth-related aggregation was based on particle density or particle number (Pn). The ratio of the particle number for either the AA-COM or the CC-COM assays, Rn, are described as.

$$\text{Rn} = \frac{\text{Pn (final)}}{\text{Pn (initial)}}.$$

However, the interpretation of the Rn findings leads to reciprocal conclusions for the two cases, because the number of particles decreases with either growth-related or equilibrium aggregation, while the number of particles increases with secondary nucleation or equilibrium disaggregation.

Table 1 Experimental parameters

Sample	CC-COM			AA-COM		
	Ca, mM	Ox, mM	σ	Ca, mM	Ox, mM	σ
CONT	0.50	0.50	1.42	0.25	0.25	0.26
Citrate, 0.4 mM	0.68	0.50	1.43	ND	ND	ND
Citrate, 6 mM	3.00	0.50	1.42	1.90	0.25	0.27
Mg^{2+}, 3 mM	0.50	0.80	1.42	0.25	0.415	0.26

The solution compositions were calculated to yield nearly equivalent supersaturations (σ) by correcting for the formation of ion pairs between citrate and Ca or Ox and Mg using the program SPEC96 (courtesy of G. Nancollas). All experiments were performed with a background buffer concentration of 150 mM NaCl, 10 mM HEPES, pH 7.5

Following logic similar to that used above for Rd, finding Rn(CC) = Rn(AA) would still indicate pure growth, while Rn(CC) > Rn(AA) would indicate secondary nucleation and Rn(CC) < Rn(AA) would indicate growth-related aggregation. Because of the larger uncertainties associated with particle number measurements, these observations were used only for qualitative confirmation of conclusions related to secondary nucleation or growth-related aggregation effects.

Crystallization modifiers tested: small molecules and macromolecules

The influences of several known inhibitors were tested in the CC-COM and AA-COM assays. Relative supersaturation, σ, was kept constant by addition of calcium ions or oxalate ions (Table 1) to offset the calculated ion complexation of sodium citrate or magnesium chloride (Sigma Chemical Co.), respectively. Homopolymers were also commercially available from Sigma and details of the composition are given in Table 2. No adjustments were made to samples based on macromolecule additions. Osteopontin (mOPN), a native protein crystal growth inhibitor isolated from mouse renal cortical collecting duct cells, was also used in these studies [31]. While anionic macromolecules are known to bind calcium ions [32, 33], the quantities of proteins added were too small to significantly affect the free calcium ion concentration at any of the conditions reported; a fact confirmed by the absence of change in calcium ion electrode signal when macromolecules were introduced into the reaction vessel.

All data were reported with standard errors, and statistical significance for comparisons was determined using Student's *t* test analysis.

Results

CC-COM: apparent crystal growth rate

Apparent crystal growth rate is the most studied parameter using constant composition methodology. A series of control experiments (no added crystallization modifiers) were performed using varied additions of calcium oxalate monohydrate (COM) seed crystal. The rate shown in Fig. 1a was determined as the mass of COM crystal formed per minute based on the rates of calcium ion delivery with the addition of 300 μg of COM seed. It has been shown previously that no two crystal preparations typically yielded crystals of identical size and therefore normalization of the data by surface area was critical [18]. We observed this in the current study with two different crystal preparations: lots 91086 and 3403. The surface area correction for lot 91086 was 1.6 m^2/g determined by particle sizing methods (confirmed as 1.5 m^2/g using gas diffusion methods). Lot 3403, however, yielded a lower surface area (1.2 m^2/g). Adjusting for the surface area resulted in a linear relationship between apparent growth rate and COM surface area added (Fig. 1b), indicating that the surface area correction was appropriate. All experiments used COM lot 91086, except for the citrate and Mg^{2+} studies where lot 3403 was used.

The titration curves illustrated in Fig. 2 provide a qualitative review of the impact of small molecule urine components and polymers on the apparent CaOx growth rate. The former group includes normal urine constituents that have been utilized therapeutically in stone disease. The latter group includes polyanions, such as pD and pE, which have traditionally been used to mimic native crystal growth inhibitor acidic proteins such as osteopontin, as well as the polycation pR which may mimic more basic urinary proteins, such as transferrin or immunoglobulins. As shown in Fig. 2a, the addition of 3 mM magnesium had no impact on the apparent growth rate, while citrate slowed the apparent growth rate in the system. The curve shapes in either case were nearly linear and similar to that of the control additions, suggesting a pure growth mechanism.

In contrast to the effect of 6 mM citrate on Ca^{2+} titration, some homopolymers impacted the shape of the curves (Fig. 2b). While the polycation pR produced a titration curve indistinguishable from a control run, single macromolecule additions of pE, pD, and mOPN (data not shown) depressed the apparent growth rates in the same manner, but to varying degrees. They produced titration runs that demonstrated accelerating rates of titrant addition as crystallization proceeded. Characteristically, polyanion experiments equilibrated within a minute of seed crystal addition, followed by reduced growth rates compared to control, which gradually increased as the reaction proceeded. This pattern would be expected in a strongly nucleating system, where growth proceeds slowly until new crystal surfaces are created through nucleation processes (presumably nuclei forming on existing crystal surfaces, or secondary nucleation). The apparent growth rate accelerates as the crystal surface area is rapidly expanded. The polyanion rich mixture of pR/pD (25:75 nM; data not shown) and the

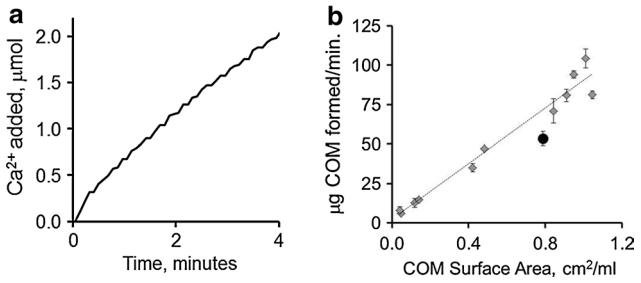

Fig. 1 CC-COM titration. **a** The figure depicts the addition of Ca^{2+} in µmoles after adding 300 µg COM seed crystal in a control (no added inhibitors) CC-COM experimental run. **b** Apparent growth rates obtained using the CC-COM plotted against varied seed crystal addition expressed in terms of COM surface area added per mL of reaction volume ($y = 88.1x + 2.4$; $R^2 = 0.97$). COM seed crystal lot 91086 is shown in *gray diamonds*, while lot 3403 is shown as a *black circle*. Each point is the average of three or more observations; standard error shown. The range of seed mass added was 15–388 µg per 5 mL reaction volume

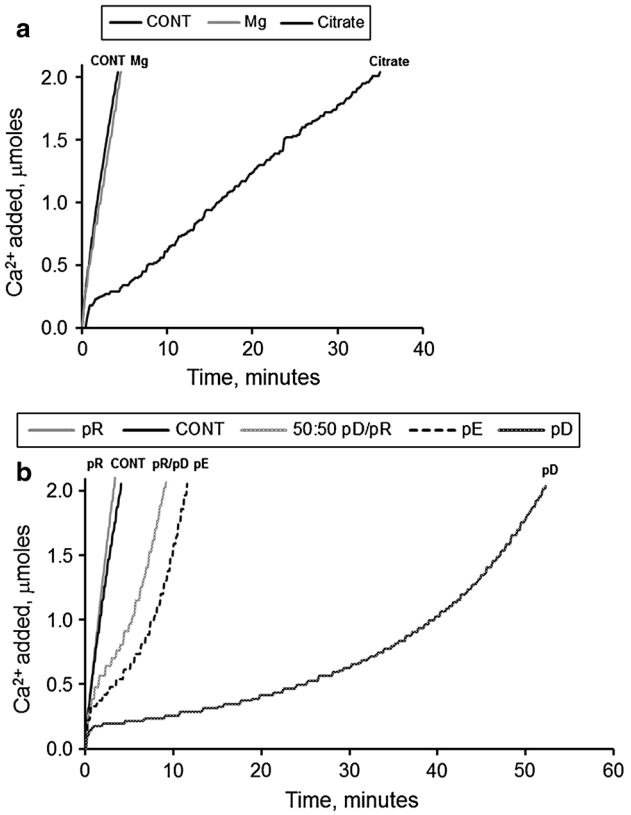

Fig. 2 Effect of small and large molecular weight additives on apparent crystal growth rate. **a** Titration curves (*left* to *right*) for CONT, 3 mM Mg^{2+}, and 6 mM citrate addition. **b** Titration curves (*left* to *right*) for pR, CONT, 50:50 pR/pD, pE, and pD. All polymers added at 100 nM. All experiments had 300 µg COM seed crystal added and were allowed to titrate until mass doubling

Table 2 Macromolecules tested

Macromolecule	Abbreviation	MW, kDa	Sigma #
Polyaspartate	pD	11.8	P5387
Polyglutamate	pE	13.6	P4636
Polyarginine	pR	11.8	P4663
Osteopontin	mOPN	32.4[a]	Cell media isolated [31]

[a] Estimated molecular weight based on amino acid sequence only (http://www.uniprot.org accession number P10923)

polyanion equivalent (50:50 nM pR/pD; Fig. 2b) produced a similar accelerating growth rate curve. In contrast, the polycation rich mixture of pR/pD (75:25 nM) and the equimolar mixture of pR/mOPN produced titration curves that resemble control experiments (data not shown), suggesting a pure growth process at these conditions.

A more quantitative review of apparent growth rate changes was obtained by calculating the percent growth rate inhibition compared to the control experiment (Table 3). The rates for conditions that yielded distinctly non-linear growth profiles were calculated as described above using simply a linear growth rate assumption. Additions of pD and pE at concentrations of 100 nM resulted in substantial apparent growth rate inhibition; 92.8 ± 1.2 and 72.1 ± 1.4 %, respectively. The polycation pR produced no apparent inhibition; 1 ± 7 % (indistinguishable from zero). Lesser amounts of pD added still achieved significant growth rate inhibition (10 and 50 nM yielded 43 and 90 % inhibition, respectively). The addition of mOPN (100 nM) yielded results similar to other polyanions tested (92.4 ± 0.9 % inhibition).

The polycation/polyanion mixtures of pR and pD demonstrated more complex behavior. Earlier aggregation studies have shown that polyarginine and polyaspartate behaved differently in combination than when added singly [27], and similar observations were noted for apparent growth rate using the CC-COM system in this study. The growth rate inhibition is plotted against the pD concentration for both the pure pD system and pR/pD mixtures in Fig. 3. With only pD added, growth rate inhibition rose rapidly from 0 at very low concentrations of pD, and appeared to be asymptotically approaching a saturation point above 90 % inhibition at the 50 nM addition. Conversely, the pR/pD mixtures data demonstrated less growth rate inhibition compared to the pure pD system, and the data suggested a transition from pR like behavior (with no significant growth rate inhibition) in the polycation-dominated mixture (75:25 nM pR/pD) to pD like behavior in the polyanion-dominant conditions (25:75 and 50:50 nM pR/pD). Surprisingly, the polycation-dominant condition (75:25 nM pR/pD) appeared to have caused growth rate acceleration, though

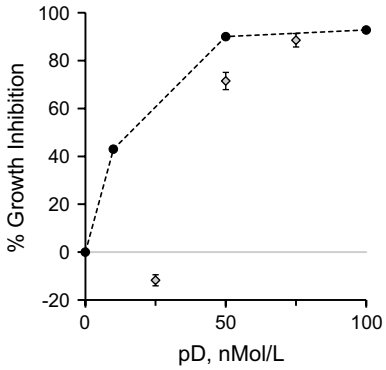

Fig. 3 Polymer mixtures and COM growth rate inhibition. The inhibition of the apparent growth rate is plotted against the pD concentration for additions of either pD alone (*black circles*) or pR/pD mixtures (*gray diamonds*) as described in the methods section. The addition of pD alone demonstrated significant inhibition of COM growth at 10 nM concentration and reached 90 % inhibition at 50 nM addition with only an incremental increase at 100 nM pD. Conversely, the pR/pD mixtures demonstrated a transition from pR-like behavior (essentially no inhibition of growth rate) at low pD concentrations (pR rich mixtures) to pD-like behavior (strong growth rate inhibition) at pD-rich conditions, approaching pD alone behavior at the 25:75 nM mixture. A 58:42 nM pR/pD mixture would contain nearly equal numbers of positive and negative charges, and the transition in COM inhibition clearly occurred close to that condition. All experiments were run in at least triplicate

the experimental conditions used in this study, designed to evaluate growth rate inhibitors, were not well suited to characterize growth rates faster than the control, limiting the reliability of this observation.

The transition from pR like behavior to pD like behavior clearly occurred at a composition between the 75:25 and 50:50 nM mixtures, and likely corresponded to expected charge equivalence point (approximately 58:42 nM pR/pD mixture) based on the differences in monomer molecular weights between R and D (156 and 115 g/mole respectively, including counterion contributions). The near equivalence of growth rate inhibition for pure pD at 50 nM to that for pR/pD at 25:75 nM suggests that the growth rate inhibition outcome for mixtures can be approximated by treating the mixture as a pure component at the concentration corresponding to the net excess of the dominant component. The equimolar mixture of mOPN and pR behaved like a polycation rich mixture; not statistically different from control, and again this mixture trended toward promoting growth, similar to the 75:25 nM pR/pD mixture.

Citrate and magnesium are thought to be small ion inhibitors of COM crystallization, and they were also tested at concentrations relevant to normal physiologic conditions. The average urine citrate concentration was reported to be 2.5 mM (range 0.4–5.8 mM), while the average urine magnesium concentration was determined to be 3.6 mM [34]. Table 4 shows the data for apparent growth inhibition for the extremes of urinary citrate (6 and 0.4 mM) and the average (3 mM) urinary magnesium concentration, while the adjustments in solution conditions required to obtain desired supersaturation in the presence of expected ion pair formation are shown in Table 1. The growth rate inhibition was 92 and 51 % for the high and low citrate concentrations, respectively; while magnesium was without significant effect. These observations are similar to the growth rate inhibition reported by Wang et al. [13] for these same inhibitors.

Particle size distributions

Crystal growth rate measurements alone would not predict the varied results seen in the particle size distributions (PSD) of CC-COM control experiments (Fig. 4a). Based on the ideal crystal growth model defined above, at mass doubling, the initial seed crystal PSD (COM Seed, dashed line) would shift slightly to the right (IDEAL, solid line), towards larger particle sizes. In the absence of exogenous substances, the addition of small amounts of COM seed crystal (15 µg) in the CC-COM system resulted in a distribution shift that was smaller than expected, suggesting that secondary nucleation was occurring at a significant rate. Greater amounts of seed crystals added resulted in increasing particle size (greater than ideal), providing evidence for growth-related aggregation. Decreases in the relative supersaturation, σ, of the growth system which decreases growth rate, also appeared to increase the growth-related aggregation in a limited set of experiments [$\sigma = 1.42$,

Table 3 Summary of CC-COM apparent growth inhibition and Rd(CC) for the macromolecules tested

Sample	Inhibition (%)	$p < 0.05$	Rd(CC)	$p < 0.05$
pD, 100 nM	92.8 ± 1.2 (5)	*§	0.68 ± 0.01	*
pE, 100 nM	72.1 ± 1.4 (4)	*¥§€	1.21 ± 0.03	¥
pR, 100 nM	1 ± 7 (3)	¥€	1.18 ± 0.04	¥
mOPN, 100 nM	92.4 ± 0.9 (2)	*§	1.02 ± 0.02	
Polymer mixtures				
pR/pD				
25:75 nM	88 ± 2 (3)	*§₹	1.23 ± 0.10	
50:50 nM	71.5 ± 1.3 (3)	*¥§€₹	1.21 ± 0.01	
75:25 nM	−11.7 ± 0.7 (3)	*¥€₹	1.22 ± 0.02	
mOPN/pR				
50:50 nM	−41 ± 9 (2)	¥€	1.14 ± 0.01	

The apparent growth rate inhibition for the CC-COM experimental runs were calculated as described in the methods section. The mean values and standard errors are reported with the number of experimental runs given in parenthesis. Statistical significance is noted when $p < 0.05$ for comparisons to control *, pD[¥], pR[§], mOPN[€]. All pR/pD mixtures were significantly different from each other[₹]. COM lot 91086 was used throughout these experiments

Table 4 Summary of CC-COM and AA-COM properties of Mg^{2+} and Citrate

Sample	CC-COM		AA-COM
	Inhibition (%)	Rd	Rd
CONT ($n = 10$)		1.05 ± 0.01	1.12 ± 0.17
Citrate, 0.4 mM (3)	51 ± 3*	$1.05 \pm 0.02^{₮}$	ND
Citrate, 6 mM (2)	92 ± 4*§	3.3 ± 0.2*§	0.84 ± 0.06*
Mg^{2+}, 3 mM (3)	$4 \pm 7^{§₮}$	$1.07 \pm 0.07^{₮}$	0.96 ± 0.16

The apparent growth rate inhibition for the CC-COM experimental runs were calculated as described in the methods section. The number of experimental runs is given in parenthesis. Mean values and standard errors are reported for both the CC-COM and AA-COM assays. Statistical significance is noted when $p < 0.05$ for comparisons to control *, 0.4 mM Citrate§ and 6 mM Citrate₮. COM lot 3403 was used throughout these experiments

0.97, and 0.50 yielded Rd(CC) values of 1.03, 1.08, and 2.44, respectively]. The ratio of particle number, Rn(CC), obtained in this series of control experiments with varied seed crystal mass additions demonstrated an increase in particle density for lower seed crystal additions and a decrease in particle density at higher seed crystal additions (Fig. 4b), supporting the conclusions from Rd(CC).

Conversely, no change in particle number was observed in the aggregation assay at these different seed crystal additions, indicating that both observations were dependent on active growth-related processes in the CC-COM system. Figure 4c shows the data for Rd(CC) plotted against Rd(AA) for this same series of control experiments with varying amounts of seed crystal added. Similar to our earlier study [27], Rd(AA) was essentially constant at all seed crystal additions, whereas Rd(CC) was clearly <1 at low seed crystal additions (15 and 37.5 µg) and >1 at high seed crystal additions (300 and 388 µg), indicating nucleation dominant conditions in the former and growth-related aggregation in the latter. This representation of the data was introduced here, because graphing the data in this manner greatly facilitates the interpretation of inhibitor effects on COM that follows.

Figure 5 shows the results from plotting Rd(CC) vs Rd(AA) from the experiments with various crystallization modifiers added, and allows us to separately account for the equilibrium aggregation or disaggregation effects of the additives and properly interpret the growth-related aggregation or secondary nucleation effects in the CC-COM system. The line of identity defines the results for ideal growth conditions for the CC-COM assay, since any equilibrium disaggregating or aggregating effects of an additive should be equivalently present in the CC-COM experiment and pure growth would produce Rd(CC) = Rd(AA). Thus, deviations of Rd(CC) from the line of identity can be readily interpreted, with Rd(CC) values below the line of identity indicating secondary nucleation (smaller than expected particles), while Rd(CC) above this line indicating growth-related aggregation (larger than expected particles).

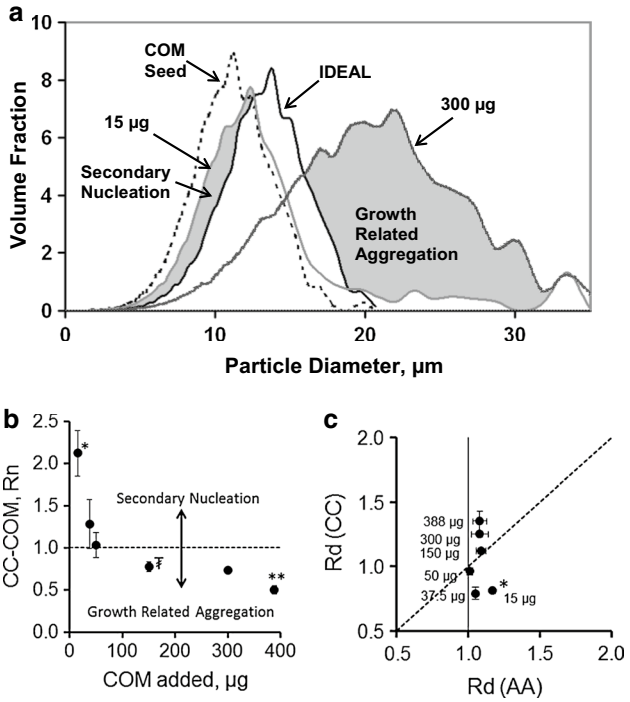

Fig. 4 Particle size distribution (PSD) analysis for control experiments. **a** PSD for CONT experiments (without macromolecule or small molecule additions). The COM seed crystal (lot 91086) is shown as a *dashed line*. The ideal mass doubling of this profile is shown in a *solid black line*. The 15 µg COM addition has a significant volume fraction that is smaller than the ideal profile, suggestive of "secondary nucleation" (*Labeled grayed area*). The 300 µg CONT experiment has a significant volume fraction that is larger than the ideal profile suggesting "growth-related aggregation" (*Labeled grayed area*). **b** Rn(CC) particle number data are shown for CONT experiments with varied seed crystal additions (*left* to *right* 15, 37.5, 50, 150, 300, and 388 µg COM). Rn(CC) = 1 is shown as a *dashed horizontal line*. Statistical comparisons ($p < 0.05$): *different from all points but 37.5 µg, **different from all other points, ₮different from all points except 50 and 300 µg. **c** A particle diameter comparison, Rd(AA) vs Rd(CC), for CONT experiments with varied seed crystal additions. Rd(AA) CONT data reported earlier [27] compared to Rd(CC) CONT data. Statistical comparisons for Rd(CC): *different from all points except 37.5 µg, all other points are significantly different from each other ($p < 0.05$)

For the pure polymer components, the polyanions (pD, pE, and mOPN) behaved similarly in that they all disaggregated the COM seed crystals in the aggregation assay, as shown in Fig. 5 by their lying to the left of the value of 1.0 on the *x*-axis, but they differed greatly in their behavior in the CC-COM assay (*y*-axis deviations in Fig. 5). Only pD exhibited a very small Rd(CC) (0.68 ± 0.01; vs. CONT, $p < 0.05$), which fell below the line of identity and indicated secondary nucleation-dominated behavior in the CC-COM assay. Osteopontin produced an Rd(CC) of 1.02 ± 0.02, which was smaller than control ($p < 0.05$), but it was still above the line of identity, consistent with growth-related aggregation as a weakly dominant process. The Rd(CC) for pE was not significantly different from control, but following adjustment for equilibrium disaggregating effects, pE demonstrated an increased propensity for growth-related aggregation, as indicated by the large deviation from the line of identity. Particle number data (Fig. 5, inset) supported these observations. All three polymers, pD, pE, and mOPN, increased particle density in the AA-COM, but pD fostered large increases in the Rn(CC), while mOPN fell on the line of identity (no clear deviation from pure growth). On the other hand, pE showed a net decrease in Rn(CC), consistent with growth-related aggregation. The polycation, pR, was not different from the control condition.

Mixtures of pR and pD promoted crystal aggregation to varying degrees in the static crystal assay (Fig. 5, *x*-axis), but in the CC-COM assay Rd(CC) values for the three mixtures (25:75, 50:50, 75:25 nM pR/pD) were not statistically different from control or each other. Real differences between these three conditions were emphasized when graphed in comparison with the AA-COM assay (Fig. 5). In this representation, the pR-rich condition (75:25) and the 50:50 mixture, which bracket the charge equivalence composition, lay in a graphical region that suggested secondary nucleation domination of the CC-COM assay superimposed on aggregation promotion in the AA-COM assay. The native macromolecule mOPN mixture with pR yielded similar values (Rd(CC) $= 1.14 \pm 0.01$; $p < 0.05$ vs. CONT) and also fell in the same area of the plot. On the other hand, the 25:75 pR/pD mixture data showed only a small difference from control, with no significant static aggregation effect but strong growth-related aggregation. The Rn data (Fig. 5, inset) yielded similar outcomes, though the 25:75 mixture deviated more substantially from the control condition in this parameter.

The small molecule inhibitors citrate and magnesium were also tested for their effects on COM aggregation (Table 4). When the solution conditions were adjusted for the known ion complexation of the additives, Mg^{2+} had no significant effect on either static or growth-related aggregation. However, citrate at high concentration (6 mM) mildly disaggregated seed crystals under static conditions,

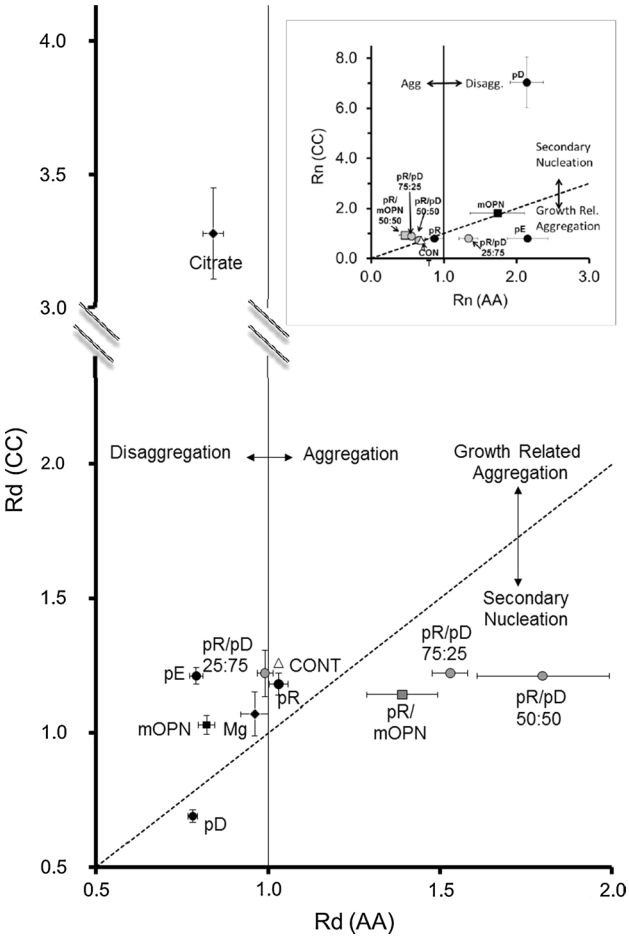

Fig. 5 Comparison of Rd(CC) and Rd(AA). The experimentally determined Rd(CC) is plotted on the *y*-axis versus the experimentally determined Rd(AA) with the same small molecule, polymer or polymer mixture on the *x*-axis (All with 300 μg seed crystal addition) [27]. The *dotted line* is the *line* of identity between the two determinations *above* and *below* which growth-related aggregation and secondary nucleation are assumed to predominate. The *vertical solid line* signifies Rd(AA) equivalent to 1. *Inset* Particle number analysis for the same experimental sets. The data for $Mg^{2+}$and citrate are not shown. In both graphs, single homopolymers are shown in *black circles*, while polymer mixtures are shown in *gray*. Osteopontin (OPN) is shown as a *black square* and a mixture of OPN with pR is shown as a *gray square*. The control ($n = 27$) is shown as an *open triangle*, while Mg^{2+} and citrate are shown as *black diamonds*. Values are the means (*n* values given in Tables 3 and 4) with the SE as *error bars*

but dramatically increased growth-related aggregation in the CC-COM assay. Interestingly, citrate at a lower concentration (0.4 mM) was not statistically different from control with respect to aggregation behavior, suggesting that the slow growth rates at 6 mM citrate were a major factor in the enhanced growth-related aggregation. Apparently, the disaggregating effects of high citrate roughly offset the growth-related aggregation effects at this condition to yield the nearly linear growth rate profile observed in Fig. 2a.

Discussion

Constant Composition assays have been studied extensively for growth rate kinetics [9–19, 21, 22, 24, 25]. We, and others, have used particle sizing technology to expand the information obtainable from this crystal growth assay to allow differentiation of concurrent nucleation and aggregation events [8, 11, 35, 36]. While all three processes (nucleation, growth, and aggregation) are probably active at all times under growth conditions, data reported here (Fig. 4) clearly demonstrated that CC-COM experiment can be configured to favor either secondary nucleation (the creation of new, smaller crystals predominating) or growth-related aggregation (the fusion of newly formed and preexisting crystals into yet larger aggregates predominating) by simply adjusting the amount of seed crystal added to initiate the reaction. The general findings that small seed crystal additions (<50 μg COM) favored secondary nucleation and large additions (>150 μg COM) favored growth-related aggregation have reproduced in greater detail the observations we reported in hydroxyapatite experiments [11], suggesting that this behavior is a general property of crystallization of calcium salts. In fact, the seed crystals (formed under high supersaturation conditions) demonstrated the consequence of growth-related aggregation when examined by electron microscopy [27], where the characteristic particles were shown to be aggregates of many incompletely oriented single crystals. A portion of this aggregation was apparently due to physical forces or surface interactions, which could be disrupted by the addition of certain chemicals, particularly anionic polymers in both this study and earlier work [27]. The inclusion of a secondary measurement of aggregation at near-equilibrium conditions Rd(AA) is a critical additional factor in isolating the various influences of these aggregation and nucleation effects in inhibitor studies, as illustrated in Figs. 4c and 5, since the reference state PSD must be appropriately adjusted for equilibrium effects before calculating growth-related changes for various additives.

Of course, some of these effects were also evident in growth rate profile deviations from linear (pure growth), as illustrated in Figs. 1a, 2a, b, where aggregation caused a decelerating rate as the reaction proceeded through annihilation of surface area with time, and nucleation caused an accelerating rate as the reaction proceeded through generation of new crystal surfaces. Unfortunately, these are indirect rather than direct observations, and the superposition of the opposing effects of simultaneous nucleation and aggregation can yield a profile with little deviation from linear response, obscuring contributions from these additional processes in the growth rate analysis. Consequently, more quantitative evaluation of the growth profiles was not pursued. It is sufficient to note that the growth profiles yielded data that were generally consistent with the more detailed particle sizing-based analyses, such as the mild degree of aggregation demonstrated by the decelerating rate in Fig. 1a for a 300 μg COM addition with no additives, or the high degree of nucleation demonstrated by the accelerating growth rates with anionic polymer additions (Fig. 2). A notable exception to these general conclusions was the growth profile for 6 mM citrate addition, which was nearly linear, despite clear evidence of a high degree of growth-related aggregation at this condition in the particle sizing data, discussed further below.

We recognize that the use of the calculated IDEAL PSD as a reference point for calculating Rd(CC) and defining changes in growth-related aggregation in comparisons of various experimental conditions is a limitation of our approach. While our approach to this calculation may be simplistic, it is straightforward, and no better alternative could realistically be considered without detailed knowledge of both the available surface area for unique crystal faces in the sample and face-specific growth rates. However, using a different calculation for the expected PSD under pure growth assumptions would only shift the "zero" point that separated conditions dominated by nucleation process from those dominated by aggregation processes. Also, the current definition was well supported by observations of Rn(CC), where the number of particles in the sample clearly increased in nucleation-dominated conditions and decreased in aggregation-dominated conditions using the current definitions.

The larger uncertainties associated with particle number determinations made Rn(CC) a less desirable parameter to monitor. Of course, use of the full PSD in comparisons between experimental conditions would be more powerful and robust, as such comparisons would differentiate between conditions with pure growth from those with varying amounts of nucleation and aggregation in balanced proportions such that Rd(CC) and Rn(CC) might be invariant. Having observed no such circumstances in this study, the remainder of the discussion will focus on comparisons of Rd(CC) and Rd(AA) to describe the modification of COM crystal growth behaviors in the presence of various small ions and ionic polymers, that provide insight into kidney stone formation.

The role of small molecules and ions was more straightforward to consider, though only a few examples were explored in this study, specifically magnesium and citrate ion additions. These small ion experiments were fundamentally different from the polymer additive experiments in that the small ion concentrations known to be relevant from studies of normal urine samples are sufficiently large that the free ion concentrations of calcium and oxalate were reduced through known ion pairing reactions with citrate and magnesium ions respectively. Consequently, substantial amounts of additional calcium chloride were required

in the citrate containing solutions to adjust them to the goal supersaturation in either AA or CC experiments. Likewise, substantial additional sodium oxalate was added to the magnesium containing samples (see Table 1) to compensate for the effect of magnesium oxalate ion pair formation on the free oxalate concentration.

When compared at constant supersaturation, magnesium ion had no effect on COM crystal growth rates or Rd values. In the clinical management of stones, increasing urinary magnesium would still be desirable through its effects in lowering supersaturation, but it appears to contribute no additional protection against crystal formation. Earlier calcium phosphate constant composition reports show that magnesium ions inhibit the crystal growth rate of some forms of calcium phosphate, but the magnesium concentrations tested were greater than 100 times those described in this report [14].

On the other hand, citrate at higher concentration had a strong inhibitory effect on crystal growth rates, as well as causing a small decrease in Rd(AA). The large increase in Rd(CC) seen with citrate was unexpected given its otherwise inhibitory properties with respect to COM crystallization, but this result appeared to be a consequence of the longer reaction times, rather than a consequence of citrate interactions with COM affecting growth-related aggregation. Unfortunately, the few experiments without additives at lower supersaturations with constant COM seed addition were not as slow as the high citrate crystallization condition, so we were unable to rule out citrate effects on growth-related aggregation.

Changes in COM growth rates, Rd(CC), and Rd(AA) induced by additions of various pure protein components (pD, pE, pR, and OPN) demonstrated a variety of behaviors. The concentration of these polymers was sufficiently low that no change in supersaturation could be anticipated based on ion pairing interactions between Ca and the polyanions or oxalate and pR, even if the small ions were bound to every possible site. This contention was supported experimentally by the observation that the Ca-selective electrode signal did not change in the CC assay upon addition of the any of the polyanions. Consequently, all of the effects observed with polymeric additives were indications of direct effects on the crystallization processes: nucleation, growth, and aggregation. The polycation, pR, addition was the simplest to describe, as pR demonstrated no significant effect on any of these measured parameters when used by itself, though it induced profound changes in behavior when mixed with polyanions, as described below. These pR results are consistent with noted lack of effect of pR on growth rate of growth hillocks on (100) and (010) faces described previously [37].

The additions of pD or pE demonstrated surprising differences in COM crystallization behavior, given the similarity of their structures. While both polyanions demonstrated similar activity with respect to disrupting crystal aggregation at near-equilibrium conditions, pD was clearly the more potent growth rate inhibitor (Fig. 2b) and blocked growth-related aggregation, whereas pE promoted growth-related aggregation, based on its relatively larger displacement from the line of identity in Fig. 5 compared to the CONT condition. While the growth profiles in Fig. 2b show similar accelerating rates for pD and pE, the particle sizing data demonstrated large differences in their interactions with COM, where secondary nucleation was a dominant process with pD addition, and growth-related aggregation was dominant with pE. Important differences clearly exist between pD and pE in their face selective interactions with COM, which are supported by several previously published observations. In particular, pE was not effective at inducing CaOx dihydrate (COD), compared to pD, but instead induced a COM aggregate morphology in bulk crystallization studies [38]. In atomic force microscopy (AFM) analyses of COM growth on selected surfaces, pE exhibited a much weaker effect than pD on the (100) surface (normally seen as the large hexagonal face in COM single crystals) and a stronger effect than pD on the (010) face (prominent side face) [37, 39]. The weak or absent interaction with (100) surface by pE likely accounts for its lack of growth-related aggregation inhibition, as the crystal aggregates seen in the seed crystals appear to be stacked on their (100) faces [27]. Conversely, pD interacted strongly at the (100) face and more strongly inhibited crystal growth in the (001) direction; the most rapid growth direction in COM based on crystal morphology [37, 39]. Also, strong interaction at the (100) face would be expected to confer strong inhibition of growth-related aggregation based on the morphology of the seed crystals [27].

The acidic protein, mOPN, exhibited intermediate behavior between pD and pE, as might be anticipated from the fact that mOPN contains a mixture of these two amino acids, along with numerous phosphorylation sites that likely affect interactions with the crystal surface. In overall growth rate inhibition, mOPN was most similar to pD, consistent with the relative preponderance of D residues compared to E residues in this protein (mOPN contains 41 D residues (13.9 %) and 27 E residues (9.2 %) of 294 total amino acids—Uniprot.org database). The near equivalence of growth rate inhibition for pD and mOPN is consistent with the relative similarity of mOPN and pD effects on COD formation [38], but addition of particle sizing data demonstrated a more nuanced picture of mOPN interactions with COM. Rd(CC) with mOPN was significantly below the control value of at 1.02, though the vertical displacement from the line of identity after adjusting for the equilibrium disaggregating effect of mOPN suggested that a similar level of growth-related aggregation occurred

under both mOPN and control conditions. The Rn plot based on particle number data (Fig. 5, inset) has mOPN right on the line of identity (same as control and pR), indicating a balance between nucleation and aggregation effects under any of these conditions. Note by comparison that pD deviated strongly in the direction of inducing secondary nucleation, while pE deviated in the growth-related aggregation direction in the Rn plot, consistent with the conclusions from Rd(CC) data above.

While the blend of D and E effects contributed by mOPN in COM crystallization has been demonstrated in these results, trying to further analyze these results on the basis of face selective interactions using data for model proteins, such as pD and pE is problematic, due to the lack of relevant data. The presence of phosphorylation sites on OPN certainly contributes an additional strong crystal surface interaction which has not been characterized in the same manner, though phosphorylation of OPN or OPN fragments has been shown to increase growth rate inhibitor properties in several studies [12, 40, 41]. There are additional data showing changes in spontaneous nucleation rates as a function of OPN phosphorylation states, but these conditions were quite different from the seeded growth CC assay in this study. Experiments using AFM have shown that OPN binds to (100) surface (pD like feature) with little effect on crystal growth on that face (pE like feature), but it demonstrated strong binding and growth inhibition interactions at the (010) face (pE like feature) [40], and these effects were influenced by phosphorylation [13]. Subsequent experiments examining the force of adhesion of chemically modified AFM probe tips showed an apparently anomalous result, where OPN added to the solution increased the adhesion force for carboxylic acid functionalized tips at the (100) surface, when other polyanions tested reduced the adhesion force [42]. The influence of the large number of uncharged residues in naturally occurring proteins has not been tested in prior experiments, though these hydrophobic residues likely contribute to protein aggregation processes that have been described [40, 43] and may contribute to interactions at COM surfaces. In summary, mOPN demonstrated a complex set of interactions at the COM surface, likely dependent on a blend of properties contributed by the various amino acid components, which has not been fully characterized to date.

Mixtures of polycations and polyanions resulted in significantly different outcomes than the addition of the macromolecules singly. In general terms, strong binding associations between polycations and polyanions were anticipated under these solution conditions, based on earlier polymer chemistry experiments [44, 45], such that these solutions are most simply understood by treating them as a mixture of polycation/polyanion aggregates with near zero net charge and excess free polyanion or polycation, depending on the composition of the mixture. The growth rate inhibition data tracked with the free polyanion composition in the pD-rich conditions (pR/pD of 25:75 and 50:50), where these compositions showed growth rate inhibition with accelerating growth rate profiles, comparable to pure pD solutions (adjusted for net free pD concentration), with no apparent effect of the polycation/polyanion aggregate on these data. Conversely, the pR-rich condition (pR/pD of 75:25) and pR/mOPN mixture showed no growth rate inhibition, similar to pR alone. In the absence of a strong inhibitor contribution from pR, a possible nucleation promoting effect of the polycation/polyanion aggregate may be evident in the apparent growth rate acceleration in these latter two samples, though the experimental conditions employed in this study made interpretation of the growth rate profile impossible due to the increased uncertainty associated with this observation. The pR/mOPN mixture may have been a nearly equal cationic and anionic charge condition, since the anionic side chains account for only a fraction of the total amino acids in mOPN. Detailed knowledge of the degree of post-translational modification (phosphorylation and glycosylation) would be required to calculate the actual charge ratio precisely, but the increase in apparent growth rate with strong secondary nucleation component (Fig. 5) suggests a dominant polycation/polyanion aggregate fraction. Earlier studies have reported promotion of COM nucleation using OPN immobilized on a substrate [46], and the polycation/polyanion aggregates in this case could functionally mimic OPN immobilized on a substrate, albeit a microscopic one.

The results from aggregation assays, Rd(CC) and Rd(AA), accentuated the effects of the polycation/polyanion aggregates on COM crystals. The induction of COM aggregation demonstrated in the AA-COM assay data for pR/pD mixtures (50:50 and 75:25) and for the pR/mOPN mixture must be related to the presence of polycation/polyanion aggregates, since each of the individual components demonstrated disaggregating effects on COM. These observations mimic the reported behavior of THP tested in vitro [43], where THP aggregation induced by desialylation, particularly at higher salt content, caused COM aggregation in an AA-COM assay, while the native THP remained molecularly dispersed and demonstrated a disaggregating effect. An earlier report has described loss of inhibitor functions with urinary protein aggregate formation [47].

The pR/pD (25:75) mixture deviated from this pattern, likely because the large excess of free pD begins to dominate the COM interactions. This sample did display significant differences from the pure pD addition indicating persistent polycation/polyanion aggregate effects, with the mixture causing almost no aggregating or disaggregating effects in Rd(AA) while still inducing growth-related aggregation [change in Rd(CC)], comparable to control.

Somewhat surprisingly, the three mixtures demonstrating aggregation promotion in the AA-COM assay appeared to be dominated by secondary nucleation in the CC-COM assay, falling well below the line of identity in Fig. 5. Similar observations were seen in the Rn data (Fig. 5, inset), though the differences appeared to be smaller by this measure. These results suggest the possibility that face involved in COM aggregation [presumably (100)] is the same in either process, such that induction of COM seed aggregation before addition of oxalate ions to the CC-COM assay precludes the possibility of growth-related aggregation. Consequently, secondary nucleation pathways appear to be enhanced, including contributions from both crystal surfaces (as seen in the control experiments) and polycation/polyanion aggregates. The large deviations from the line of identity observed for these 3 samples in Fig. 5 suggest that the latter contribution was strongly dominant.

In conclusion, the addition of particle sizing analysis to CC experiments in COM crystallization has demonstrated the importance of both nucleation and aggregation processes occurring concurrently with growth similar to results obtained in hydroxyapatite crystallization [11], with nucleation processes favored at low seed crystal densities and growth-related aggregation at high seed crystal densities. Experiments to characterize the effects of various putative CaOx kidney stone inhibitors demonstrated a complex array of effects. Experiments with putative small ion inhibitors, magnesium and citrate ions, showed that both ions exerted influence on COM crystallization by lowering the supersaturation through known ion pairing interactions, while citrate had an additional strong inhibitory effect on COM growth rate without inhibiting growth-related aggregation. Individual proteins tested showed that polyanions were potent inhibitors of growth rate, but the cationic protein, pR, had no significant effect. The addition of particle sizing data revealed large differences between pD, pE, and mOPN, with pD pushing the system toward nucleation, pE pushing toward aggregation, and mOPN demonstrating intermediate behavior. Creating mixtures of pR with polyanions (pD and mOPN) attenuated the effect of polyanions on growth rate, but introduced additional aggregation and nucleation behaviors which were likely due to the formation of polycation/polyanion aggregates in these samples.

Acknowledgments We gratefully acknowledge the primary financial support provided in part by Merit Review and Career Development Awards from the United States (U.S.) Department of Veterans Affairs Biomedical Laboratory Research and Development Program (9305) and by The Medical College of Wisconsin (JAW). Additional financial support was provided in part by the National Institutes of Health/National Institute for Diabetes, Digestive, and Kidney Diseases (DK 48504) (JGK). We also gratefully acknowledge the technical support from Dr. Neil Mandel and coworkers at the VA National Crystal Identification Center, Milwaukee, WI, where crystal surface area measurements were performed by Dr. John Weissner and x-ray crystallography was performed by Ms. Kathy Fryjoff.

Conflict of interest The authors have no conflicts of interest to report.

References

1. Worcester EM, Beshensky AM, Hung L (1993) Nephrocalcin (NC) levels and calcium oxalate (CaOx) crystal growth inhibition in the urine of hypercalciuric and normocalciuric calcium stone formers (SF). J Amer Soc Neph 4:716
2. Ryall RL, Hibberd CM, Mazzachi BC, Marshall VR (1986) Inhibitory activity of whole urine: a comparison of urines from stone formers and healthy subjects. Clin Chim Acta 154:59–67
3. Romberg RW, Werness PG, Riggs BL, Mann KG (1986) Inhibition of hydroxyapatite crystal growth by bone-specific and other calcium-binding proteins. Biochemistry (NY) 25:1176–1180
4. Donnelly R, Boskey A (1989) The effect of gallium on seeded hydroxyapatite growth. Calcif Tissue Int 44:138–142
5. Dominguez-Vera JM, Gautron J, Garcia-Ruiz JM, Nys Y (2000) The effect of avian uterine fluid on the growth behavior of calcite crystals. Poult Sci 79:901–907
6. Falini G, Albeck S, Weiner S, Addadi L (1996) Control of aragonite or calcite polymorphism by mollusk shell macromolecules. Science 271:67–69
7. Kavanagh JP (2006) In vitro calcium oxalate crystallisation methods. Urol Res 34:139–145
8. Saw NK, Rao PN, Kavanagh JP (2008) A nidus, crystalluria and aggregation: key ingredients for stone enlargement. Urol Res 36:11–15
9. Tomson MB, Nancollas GH (1978) Mineralization kinetics: a constant composition approach. Science 200:1059–1060
10. Amjad Z, Koutsoukos P, Tomson MB, Nancollas GH (1978) The growth of hydroxyapatite from solution. A new constant composition method. J Dent Res 57:909
11. Beshensky AM, Wesson JA, Worcester EM, Sorokina EJ, Snyder CJ, Kleinman JG (2001) Effects of urinary macromolecules on hydroxyapatite crystal formation. J Am Soc Nephrol 12:2108–2116
12. Pampena DA, Robertson KA, Litvinova O, Lajoie G, Goldberg HA, Hunter GK (2004) Inhibition of hydroxyapatite formation by osteopontin phosphopeptides. Biochem J 378:1083–1087
13. Wang L, De Yoreo JJ, Guan X, Qiu SR, Hoyer JR, Nancollas GH (2006) constant composition studies verify the utility of the Cabrera-Vermilyea (C-V) model in explaining mechanisms of calcium oxalate monohydrate crystallization. Cryst Growth Des 6:1769–1775
14. Salimi MH, Heughebaert JC, Nancollas GH (1985) Crystal growth of calcium phosphates in the presence of magnesium ions. Langmuir 1:119–122
15. Koutsoukos P, Amjad Z, Tomson MB, Nancollas GH (1980) Crystallization of calcium phosphates. A constant composition study. J Am Chem Soc 102:1553–1557
16. Heughebaert JC, Nancollas GH (1984) Kinetics of crystallization of octacalcium phosphate. J Phys Chem 88:2478–2481
17. Amjad Z (1991) Inhibition of calcium fluoride crystal growth by polyelectrolytes. Langmuir 7:2405–2408
18. Kazmierczak TF, Tomson MB, Nancollas GH (1982) Crystal growth of calcium carbonate. A controlled composition kinetic study. J Phys Chem 86:103–107
19. Gebrehiwet TA, Redden GD, Fujita Y, Beig MS, Smith RW (2012) The Effect of the CO^{32-} to Ca^{2+} Ion activity ratio on

calcite precipitation kinetics and Sr^{2+} partitioning. Geochem Trans 13:1–11
20. Manoli F, Dalas E (2002) The crystallization of calcium carbonate on sodium cholate. J Mater Sci Mater Med 13:69–73
21. Lanzalaco AC, Sheehan ME, White DJ, Nancollas GH (1982) The mineralization inhibitory potential of urines: a constant composition approach. J Urol 128:845–849
22. Lanzalaco AC, Singh RP, Smesko SA, Nancollas GH, Sufrin G, Binette M, Binette JP (1988) The influence of urinary macromolecules on calcium oxalate monohydrate crystal growth. J Urol 139:190–195
23. White DJ, Coyle-Rees M, Nancollas GH (1988) Kinetic factors influencing the dissolution behavior of calcium oxalate renal stones: a constant composition study. Calcif Tissue Int 43:319–327
24. Sheehan ME, Nancollas GH (1980) Calcium oxalate crystal growth. A new constant composition method for modelling urinary stone formation. Invest Urol 17:446–450
25. Nancollas GH, Singh RP (1987) In vitro system for calcium stone formation: the constant composition model. Contrib Nephrol 58:49–58
26. Blomen LJMJ, Will EJ, Bijvoet OLM, van der Linden H (1983) Growth kinetics of calcium oxalate monohydrate: II. The variation of seed concentration. J Cryst Growth 64:306–315
27. Wesson JA, Ganne V, Beshensky AM, Kleinman JG (2005) Regulation by macromolecules of calcium oxalate crystal aggregation in stone formers. Urol Res 33:206–212
28. Howard JE, Thomas WC Jr, Barker LM, Smith LH, Wadkins CL (1967) The recognition and isolation from urine and serum of a peptide inhibitor to calcification. Johns Hopkins Med J 120:119–136
29. Dent CE, Sutor DJ (1971) Presence or absence of inhibitor of calcium-oxalate crystal growth in urine of normals and of stone formers. Lancet 775–778
30. Robertson WG, Peacock M, Nordin BEC (1973) Inhibitors of the growth and aggregation of calcium oxalate crystals in vitro. Clin Chim Acta 43:31–37
31. Worcester EM, Blumenthal SS, Beshensky AM, Lewand DL (1992) The calcium oxalate crystal growth inhibitor protein produced by mouse kidney cortical cells in culture is osteopontin. J Bone Miner Res 7:1029–1036
32. Manning G (1969) Limiting laws and counterion condensation in polyelectrolyte solutions I colligative properties. J Chem Phys 51:924
33. Veis A (1970) Biological polyelectrolytes. Biological Macromolecules Series. vol 3. Marcel Dekker, NY
34. Lemann J Jr, Pleuss JA, Worcester EM, Hornick L, Schrab D, Hoffmann RG (1996) Urinary oxalate excretion increases with body size and decreases with increasing dietary calcium intake among healthy adults. Kidney Int 49:200–208
35. Cao LC, Deng G, Boeve ER, de Bruijn WC, de Water R, Verkoelen CF, Romijn JC, Schroder FH (1996) Zeta potential measurement and particle size analysis for a better understanding of urinary inhibitors of calcium oxalate crystallization. Scan Microsc 10:401–411
36. Boeve ER, Cao LC, Deng G, de Bruijn WC, Schroder FH (1996) Effect of two new polysaccharides on growth, agglomeration and zeta potential of calcium phosphate crystals. J Urol 155:368–373
37. Jung T, Sheng X, Choi CK, Kim WS, Wesson JA, Ward MD (2004) Probing calcium oxalate monohydrate crystal growth and the role of macromolecular additives with in situ atomic force microscopy. Langmuir 20:8587–8596
38. Wesson JA, Worcester EM, Kleinman JG (2000) Role of anionic proteins in kidney stone formation: interaction between model anionic polypeptides and calcium oxalate crystals. J Urol 163:1343–1348
39. Guo S, Ward MD, Wesson JA (2002) Direct visualization of calcium oxalate monohydrate crystallization and dissolution with atomic force microscopy and the role of polymeric additives. Langmuir 18:4284–4291
40. Qiu SR, Wierzbicki A, Orme CA, Cody AM, Hoyer JR, Nancollas GH, Zepeda S, De Yoreo JJ (2004) Molecular modulation of calcium oxalate crystallization by osteopontin and citrate. Proc Natl Acad Sci USA 101:1811–1815
41. Chien YC, Masica DL, Gray JJ, Nguyen S, Vali H, McKee MD (2009) Modulation of calcium oxalate dihydrate growth by selective crystal-face binding of phosphorylated osteopontin and polyaspartate peptide showing occlusion by sectoral (compositional) zoning. J Biol Chem 284:23491–23501
42. Sheng X, Jung T, Wesson JA, Ward MD (2005) Adhesion at calcium oxalate crystal surfaces and the effect of urinary constituents. Proc Natl Acad Sci USA 102:267–272
43. Viswanathan P, Rimer JD, Kolbach AM, Ward MD, Kleinman JG, Wesson JA (2011) Calcium oxalate monohydrate aggregation induced by aggregation of desialylated Tamm-Horsfall protein. Urol Res. doi:10.1007/s00240-010-0353-7
44. Bitton R, Schmidt J, Biesalski M, Tu R, Tirrell M, Bianco-Peled H (2005) Self-assembly of model DNA-binding peptide amphiphiles. Langmuir
45. Priftis D, Laugel N, Tirrell M (2012) Thermodynamic characterization of polypeptide complex coacervation. Langmuir. doi:10.1021/la302729r
46. Umekawa T, Iguchi M, Kurita T (2001) The effect of osteopontin immobilized collagen granules in the seed crystal method. Urol Res
47. Scurr DS, Robertson WG (1986) Modifiers of calcium oxalate crystallization found in urine. III. Studies on the role of Tamm-Horsfall mucoprotein and of ionic strength. J Urol 136:505–507